Received: 14 July 2020 | Revised: 12 August 2020 | Accepted: 17 August 2020

DOI: 10.1111/fog.12499

ORIGINAL ARTICLE

FISHERIES OCEANOGRAPHY WILEY

Interannual variation in the coastal distribution of a juvenile gadid in the northeast Pacific Ocean: The relevance of wind and effect on recruitment

Matthew T. Wilson | Ned Laman

Alaska Fisheries Science Center, National Marine Fisheries Service, Seattle, WA, USA

Correspondence
Matthew T. Wilson, Alaska Fisheries Science Center, National Marine Fisheries Service, 7600 Sand Point Way NE, Seattle, WA 98115, USA.
Email: matt.wilson@noaa.gov

Abstract

Drift of propagules occurs within many populations inhabiting flow fields. This affects the number of propagules that rejoin their source population (recruitment) and plays a role in adaptive spatial redistribution. We focus on the cause and consequence of interannual variation in geographic distribution of population density among five cohorts of young-of-the-year (age-0) juvenile walleye pollock *Gadus chalcogrammus* in the western Gulf of Alaska (GOA). The coastal GOA is a wind-driven advective system. Walleye pollock spawn during spring and their eggs and larvae drift southwestward; by late summer, age-0 juveniles are variously distributed over the shelf. We found that high population densities of age-0 juveniles (ca. 6 months old) near the southwestward exit of the Alaska Coastal Current from the GOA corresponded with high abundance of larvae from the major spawning area upstream, but did not translate into high abundance at older ages. Further, offshore and upwelling-favorable winds were associated with the high downstream abundance and presumed export. In contrast, downwelling-favorable (northeasterly) wind during and shortly after spawning (April–May) was associated with high recruitment at age 1. Finally, we found that recruitment also increased with apparent retention of age-0 juveniles in favorable habitat upstream near the main spawning area. We hypothesize that wind-related retention in superior upstream habitat favors recruitment. Our results argue for including wind-driven transport in future walleye pollock recruitment models. We encourage more work on the juvenile stage of marine fishes aimed at understanding how transport and species-specific habitat suitability interact to affect population response to large-scale forcing.

KEYWORDS

advection, *Gadus chalcogrammus*, Gulf of Alaska, habitat suitability, population density, retention, Walleye pollock

[Correction added on 4 December 2020, after first online publication: the equations have been modified under section 2.4.]

1 | INTRODUCTION

Variation in downstream drift of propagules has been demonstrated for many populations inhabiting flow fields, but how might this affect the number of propagules that rejoin their source population (recruitment)? Hypotheses developed in fishery oceanography state that drift from spawning grounds is a factor in whether early life stages rear in recruitment-favorable areas (Hare, 2014; Huse, 2016). The hypotheses recognize meteorological influence on hydrography and biology (e.g., Aberrant Drift Hypothesis; Houde, 2008). However, system dynamics are complex (Bailey, Ciannelli, Bond, Belgrano, & Stenseth, 2005) and correlative relationships are sensitive to changes in basin-scale atmospheric patterns (Litzow et al., 2019), which underscores the importance of mechanistic understanding. Conceptually, the transport of propagules across unequal habitats is an important population and ecosystem dynamic because species requirements (e.g., Doyle et al., 2019; Shanks & Eckert, 2005) interact with climate and ocean currents to dynamically redistribute populations across suitable habitat (Sorte, 2013).

One relevant component of meteorology is wind. As a driver of ocean circulation, wind (speed, direction, and duration) has most recently been associated with the recruitment of snapper (*Lutjanus carponotatus*) larvae to coral reefs (Schlaefer, Wolanksi, Lambrechts, & Kingsford, 2018) and retention of cod (*Gadus morhua*) larvae along the Norwegian coast (Endo, Vikebø, Yaragina, Hjøllo, & Stige, 2020). In the Gulf of Alaska (GOA), wind was related to survival and transport of larval walleye pollock (*Gadus chalcogrammus*) (Bailey, Bond, & Stabeno, 1999; Bailey, Canino, Napp, Spring, & Brown, 1995). Multivariate models of GOA walleye pollock recruitment included wind as an indicator of turbulent mixing (i.e., wind speed cubed), which relates to larval feeding success (Porter et al., 2005), but did not include it as a driver of transport (see Bailey, Zhang, Chan, Porter, & Dougherty, 2012; Ciannelli, Bailey, Chan, Belgrano, & Stenseth, 2005; Lee, Megrey, & Macklin, 2009).

In the GOA, flow over the continental shelf is generally southwestward with substantial bathymetric influence (Figure 1). The Alaska Coastal Current (ACC) is the main circulation feature over the shelf. Flow along the slope is dominated by the Alaskan Stream, a rapid boundary current (Stabeno et al., 2004). The ACC is structured and driven by freshwater runoff and wind. The freshwater influence gives the ACC its signature low-salinity core evident as a wedge of fresher water along the coast with downwelling-favorable winds steepening the shoreward-sloping isohalines (Rogers-Cotrone, Yankovsky, & Weingartner, 2008; Stabeno et al., 2016; Yankovsky, Maze, & Weingartner, 2010). From winter to summer, the southerly and easterly winds that drive downwelling weaken and become more variable with intermittent upwelling driven by northerlies and westerlies (Stabeno et al., 2004).

Walleye pollock is a highly fecund, semi-pelagic schooling gadid of considerable economic value (Dorn et al., 2018). Its life history consists of pelagic spawning of planktonic eggs (Blood, Matarese, & Yoklavich, 1994) and larvae that transition to young-of-year (age-0) juveniles over their first summer (Brown, Mier, & Busby, 2001) after which they move toward adult aggregations (Brodeur & Wilson, 1996). The cues directing this movement are unknown. Spatially, walleye pollock occur throughout the coastal GOA, but are more abundant in the west than east (Brodeur & Wilson, 1996; Doyle & Mier, 2016; Meuter & Norcross, 2002). The largest spawning aggregation occurs in the Shelikof Strait sea valley during March and produces very high densities of eggs at depth that can be tracked spatially during development. After the ~2 week, temperature-dependent egg development period, larvae quickly ascend to 0–50 m depth (Kendall, Incze, Ortner, Cummings, & Brown, 1994). In near-surface waters, larvae can be: (a) concentrated in retention areas along the coast by downwelling-favorable wind (Stabeno, Schumacher, Bailey, Brodeur, & Cokelet, 1996), (b) advected offshore by upwelling-favorable wind where more rapid southwestward transport is possible (Bailey et al., 1995; Hinckley, Bailey, Picquelle, Schumacher, & Stabeno, 1991; Hinckley, Bailey, Picquelle, Yoklavich, & Stabeno, 1993), or (c) "anomalously" transported around Kodiak Island as predicted from biophysical modeling (Hinckley, Hermann, Mier, & Megrey, 2001) possibly in association with variation in transport (Bailey et al., 1999; Bailey & Macklin, 1994; Incze, Kendall, Schumacher, & Reed, 1989).

By late summer, age-0 juveniles are common throughout the western GOA; however, the geographic distribution of population density varies from year to year. For example, the late-summer age-0 distribution of the 1987 year class differed from the 1988 year class due to high abundances only southwest of the Shumagin Islands as opposed to also around Kodiak Island (Wilson, 2000). The abundance southwest of the Shumagins during 1987 can be attributed to downstream transport from the Shelikof spawning area (Hinckley et al., 1991). High abundance around Kodiak Island during 1988 is less certainly explained (Wilson, 2000). This variation in distribution is relevant to recruitment for two reasons: (1) the Kodiak Island vicinity supports a rich prey field that benefits juvenile body size and condition (Buchheister, Wilson, Foy, & Beauchamp, 2006; Wilson, 2000; Wilson, Mier, & Jump, 2013) and (2) individuals southwest of the Shumagin Islands are more vulnerable to export from the GOA based on model-based estimates of adult–juvenile spatial connectivity (Parada et al., 2016). In fact, the relatively high age-0 population density around Kodiak Island during 1988 was associated with relatively strong subsequent recruitment (Wilson, 2000). Since 1987 and 1988, three more year classes of age-0 juveniles have been extensively surveyed (2013, 2015, and 2017). Considerable geographic variation in distribution is evident (Rogers, Wilson, & Porter, 2019), but has not been investigated. Our goal was to examine the geographic distribution of age-0 juvenile population density for these five-year classes to better understand possible underlying cause(s) and the implication for recruitment variability. We focus here on wind as a relevant factor.

We established three objectives. Our first objective was to examine the five age-0 geographic distributions for evidence consistent with the expectation that high abundance southwest of the Shumagin Islands reflects high abundance of larvae in the Shelikof spawning area and does not translate into high abundance at older ages, due possibly to export (Parada et al., 2016). Our second objective was to determine if surface wind can reasonably explain the observed variation in

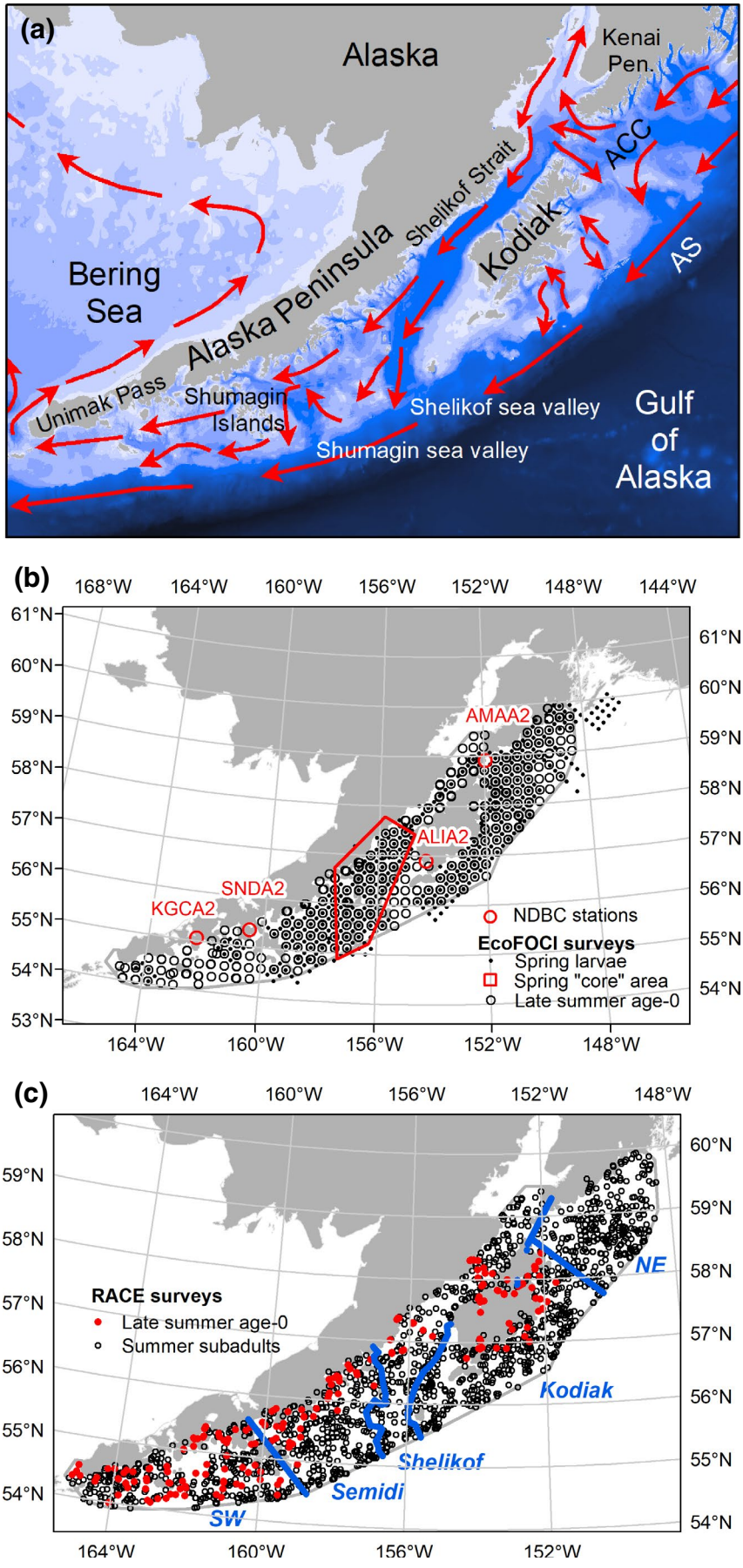

FIGURE 1 (a) Generalized flow over and along the shelf in the western Gulf of Alaska (Reed & Schumacher, 1986) (ACC, Alaska Coastal Current; AS, Alaskan Stream). (b) Location of EcoFOCI stations sampled during spring (larval walleye pollock, red polygon represents the "core" area) and late summer (age-0 juveniles) in 2013, 2015, and 2017. The four National Data Buoy Center sites are also shown. (c) Location of RACE stations sampled during late summer 1987 and 1988 (age-0 juveniles) and during summer bottom-trawl surveys during 1990, 2015, 2017, and 2019. Blue lines and labels depict the geographic stratification scheme. Gray polygon encompasses all age-0 collection sites (EcoFOCI and RACE) [Colour figure can be viewed at wileyonlinelibrary.com]

age-0 geographic distribution. We focused on surface wind as a relevant factor given its role in driving transport (Stabeno et al., 2004) and its presumed role in the downstream movement of eggs, larvae, and juveniles (e.g., Hinckley et al., 1991). Because of this focus, we relied heavily on the three most recent years when the age-0 distributions were paired with empirical surface wind data. Our decision to use only empirical wind measurements reduced sample size but avoided uncertainty about the representativeness of model-based wind in coastal areas (Ladd & Bond, 2002; Stabeno et al., 2016). Our third objective was to statistically examine the relationships between surface wind, age-0 distribution, and recruitment. Due to data constraints, we were able to robustly test only the wind–recruitment and distribution–recruitment relationships.

2 | MATERIALS AND METHODS

2.1 | Study area

The study area covers the continental shelf from Kenai Peninsula to Unimak Pass (Figure 1). The nearshore extent is bounded by shallows and non-navigable areas along a convoluted coastline. High bathymetric relief is due to islands, offshore banks, and sea valleys. Sea valleys extend across the shelf from nearshore to the continental slope and facilitate at-depth influxes of oceanic water (Mordy et al., 2019). There are three bifurcations in the ACC as it passes through our study area. The first is at the northeast entrance to Shelikof Strait, between Kenai Peninsula and Kodiak Island Archipelago (Figure 1a) where most ACC water enters the Strait but some is diverted south around Kodiak Island (Stabeno et al., 2016). The other two are partial southward diversions along the western edge of the Shelikof and Shumagin sea valleys.

2.2 | Fish distribution

To test the expectation that high abundance southwest of the Shumagin Islands reflects high abundance of larvae in the Shelikof spawning area and does not translate into high abundance at an older age, we compared region-specific age-0 abundance to the abundance of Shelikof larvae and to abundance as subadults (age 2 or 3 years old). Population density estimates of larvae, age-0

TABLE 1 Data for estimating life stage-specific walleye pollock population density were from research cruises conducted by AFSC programs in the western coastal Gulf of Alaska

Life stage	Program	Cruise	Vessel	Cruise dates			Year class	Trawl hauls	CTD casts
				Start	End	Year			
Larva	EcoFOCI	MF87-06	Miller Freeman	May 18	May 29	1987	1987	—[a]	—[b]
Larva	EcoFOCI	MF88-06	Miller Freeman	May 20	June 6	1988	1988	—[a]	—[b]
Larva	EcoFOCI	DY13-06	Oscar Dyson	May 17	June 1	2013	2013	—[a]	217
Larva	EcoFOCI	DY15-05	Oscar Dyson	May 15	June 4	2015	2015	—[a]	273
Larva	EcoFOCI	DY17-05	Oscar Dyson	May 12	June 1	2017	2017	—[a]	266
Age-0	RACE	198703	Alaska	August 12	September 20	1987	1987	118	—[b]
Age-0	RACE	198803	Alaska	August 18	September 10	1988	1988	78	—[b]
Age-0	EcoFOCI	DY13-08	Oscar Dyson	August 17	September 17	2013	2013	224	217
Age-0	EcoFOCI	NW15-01L2A	Northwest Explorer	August 8	August 23	2015	2015	70	67
Age-0	EcoFOCI	DY15-07	Oscar Dyson	August 21	September 2	2015	2015	74	71
Age-0	EcoFOCI	DY17-07	Oscar Dyson	August 22	September 14	2017	2017	127	127
Subadult	RACE-GAP	199001	Pat San Marie	June 11	August 26	1990	1987 and 1988	210	—[b]
Subadult	RACE-GAP	199001	Green Hope	June 17	September 9	1990	1987 and 1988	191	—[b]
Subadult	RACE-GAP	201501	Sea Storm	June 2	July 21	2015	2013	191	—[b]
Subadult	RACE-GAP	201501	Alaska Provider	June 1	July 20	2015	2013	176	—[b]
Subadult	RACE-GAP	201501	Cape Flattery	June 26	August 1	2015	2013	120	—[b]
Subadult	RACE-GAP	201701	Sea Storm	June 2	July 20	2017	2015	175	—[b]
Subadult	RACE-GAP	201701	Ocean Explorer	June 4	July 22	2017	2015	153	—[b]
Subadult	RACE-GAP	201901	Sea Storm	May 30	July 18	2019	2017	174	—[b]
Subadult	RACE-GAP	201901	Ocean Explorer	May 29	July 17	2019	2017	164	—[b]

Note: Cruise dates, the year class targeted in the present study, and the number of samples (trawl hauls) and hydrographic (CTD) casts are included.

[a]Population density estimates for larvae in the Shelikof core area were from L. Rogers (Dougherty et al., 2019).

[b]Hydrographic casts were not routinely conducted or were insufficient in spatial coverage on these cruises.

TABLE 2 Each study objective was addressed by analyzing series of suitable data with years representing availability (see text)

Objective	Analysis	Years
Fish distribution	Larva—age-0 juvenile	1987, 1988, 2013, 2015, 2017
	Age-0 juvenile—subadult	1987, 1988, 2013, 2015, 2017
Wind and salinity		2013, 2015, 2017
Recruitment (age-1 abundance)	*Recruitment—wind*	
	Recruitment—AMAA2	2004–2006, 2009–2017
	Recruitment—KGCA2	2009–2015
	Recruitment—SNDA2	2009–2013, 2015–2017
	Recruitment—ALIA2	2011–2017
	Recruitment—age-0 juvenile	1987, 1988, 2013, 2015, 2017

juveniles, and subadults were obtained from field surveys conducted by the Alaska Fisheries Science Center (AFSC) (Table 1). In this study, we focused on the year classes that were most extensively surveyed geographically as age-0 juveniles: 1987, 1988, 2013, 2015, and 2017 (Table 2).

2.2.1 | Shelikof larvae

The Ecosystems and Fisheries-Oceanography Coordinated Investigations (EcoFOCI) Program conducts an ongoing multidisciplinary survey of larval walleye pollock in the western GOA during spring (May–June). The core area of the sampling grid encompasses the lower Shelikof sea valley (Figure 1b). At each site, a bongo-profiler array was used to collect ichthyoplankton and hydrographic measurements over an oblique towpath. Maximum tow depth was to 100 m depth or, if shallower bottom depth, 10-m off bottom (Rogers & Dougherty, 2019); sampling occurred where bottom depth was greater than about 40 m due to ship navigation concerns. Population density estimates (number of larvae 10 m^{-2}) in the core area were estimated by Dougherty, Deary, and Rogers (2019) and obtained from L. Rogers (AFSC, pers. commun.). Hereafter, we refer to these as Shelikof larvae.

2.2.2 | Age-0 juveniles

Age-0 juvenile population density estimates were obtained from small-mesh trawl surveys conducted by the AFSC during late summer (August–September) when the year class was about 6 months old (i.e., not yet part of the adult population). Trawls used in these surveys were equipped with a 3-mm mesh liner inserted into the codend. Survey coverage was not consistent among years. We selected five years with the most extensive geographic coverage. Data for 1987 and 1988 were from discontinued surveys that were conducted by the Resource Assessment and Conservation Engineering (RACE) Division. Data for 2013, 2015, and 2017 were from ongoing EcoFOCI late-summer surveys. Regardless of survey, age-0 juveniles were distinguished at sea from older individuals by body length (Wilson, 2000, 2009).

The selected RACE survey data covered the continental shelf from around Kodiak Island to Unimak Pass (Figure 1c). Samples were collected by targeting echolayers with a small-mesh, high-opening shrimp trawl. Estimates of population density (number of juveniles m^{-3}) were from Wilson (2000), which provides additional sampling detail.

The EcoFOCI late-summer surveys were multidisciplinary and the selected data covered much of the western GOA (Figure 1b); a small-mesh mid-water trawl was used to collect age-0 juveniles and other small neritic animals. At predetermined gridded sites, as during the spring survey, a bongo-profiler array was used to collect zooplankton and record water temperature and salinity. The towpath for both gear types was oblique to a maximum depth of 200 m or, if shallower bottom depth, 15 m off bottom); bottom depth at the shallowest site sampled was 25 m. Population density (number of juveniles m^{-3}) at each site was the number of individuals collected divided by filtered water volume, which was calculated by multiplying distance fished and trawl mouth area (Wilson, 2009).

2.2.3 | Subadults

Subadult refers to age-2 and age-3 fish whose population densities were estimated using data from summer bottom-trawl surveys of groundfish. These ages were considered to be post-recruitment because Dorn et al. (2018) use age-1 abundance to index recruitment. These were conducted by the RACE Division's Groundfish Assessment Program (GAP). A standardized poly-Nor'eastern high-opening bottom trawl was used to sample groundfish over a stratified-random survey design (von Szalay & Raring, 2018). Data from the 1990 survey were used to estimate population density of the 1987 and 1988 year classes at age 3 (there was no survey in 1989) and age 2, respectively. Conceivably, adjacent year classes interact, although we have no evidence of this potential. The 2015, 2017, and 2019 surveys were used to estimate the population density of the 2013, 2015, and 2017 cohorts at age 2, respectively. Age-specific population density (number km^{-2}) in each haul (D_h) was calculated as:

$$D_h = \sum_l \left(\mathrm{CPUE}_h \frac{n_{hl}}{N_h} Y_l \right),$$

where CPUE_h is the total count of walleye pollock standardized by area swept during haul h, n_{hl} is fish count in haul h at body length l measured to the nearest cm, N_h is total number of walleye pollock measured in haul h, and Y_l is the proportion of age-2 fish (age 3 for the 1987 year class) at length (age composition). Age composition was based on otolith-aged fish from all four surveys combined and expressed as the

proportion of fish at age by cm-length bin. Aging was conducted by the AFSC Age and Growth Program (Matta & Kimura, 2012).

2.2.4 | Analysis

We geographically stratified the age-0 density estimates for comparison, first to larval abundance in the Shelikof core area for evidence of downstream movement, and then to regional abundance of subadults for evidence consistent with downstream loss (e.g., export). To stratify the data, five regions were delineated on the basis of survey coverage, oceanography (Stabeno et al., 2004), and walleye pollock demography (Figure 1c). The NE Region is the area northeast of where the ACC bifurcates to flow around Kodiak Island. It was not covered during the RACE age-0 surveys and was thus omitted from further statistical consideration. The Kodiak Region is less influenced by the ACC than by influxes of oceanic water, which was associated with food-related benefit to juvenile walleye pollock (Wilson et al., 2013). The Shelikof Region is characterized by high volume of ACC water that stimulates estuarine-like flow of oceanic influx at depth along the eastern side of the sea valley; it encompasses the major walleye pollock spawning area. The Semidi Region straddles Semidi Bank over and around which ACC flow is reduced and age-0 juveniles tend to have lower body condition (Buchheister et al., 2006) and not mix with their Kodiak counterparts (Hinckley et al., 2001; Wilson, Dougherty, Matta, Mier, & Miller, 2018). Finally, the SW Region extends from the ACC bifurcation at the Shumagin Islands to Unimak Pass where ACC water exits the coastal GOA.

The effect of region on relationships of population density between ages was assessed statistically; however, only five-year classes were included in the analysis so we additionally conducted a power analysis. A least-squares linear multiple regression model (*lm* function, R version 3.6.1, R Core Team, 2019) was fitted to the data:

$$D_{2yr} = b_0 + b_1 D_{1yr} + b_2 \text{Region} + b_3 D_{1yr} \text{Region} + \varepsilon,$$

where D_1 and D_2 denote annual estimates of mean population density at younger and older stages, respectively, of year class *y* and for region *r*, and *Region* (Kodiak, Shelikof, Semidi, and SW). The interaction term, D_{1yr}Region, allows the slope of the relationship to vary by region. Two separate analyses were conducted: (1) regression of larva (younger) and age-0 juvenile (older) abundance and (2) regression of age-0 juvenile (younger) and subadult (older) abundance. For the larva–juvenile regression, D_{1yr} simplifies to D_{1y} because the annual mean density of larvae was for the Shelikof core area (i.e., larval abundance was not geographically stratified). Population density estimates were 4th-root-transformed so that error (ε) was normally distributed; the transformation approximates a log transformation without requiring addition of a constant to null estimates. Model terms were evaluated in R (version 3.6.1; R Core Team, 2019) using Type III sum of squares (*Anova*, *car* package) (Fox & Weisberg, 2019) and sum-to-zero contrasts. A power analysis was conducted for conclusions of no significant ($p > .05$) interaction (D_{1yr}Region). Power of the slopes heterogeneity test was estimated using the exact power function of Shieh (2019), which accounts for stochasticity in predictor variables.

2.3 | Wind and salinity

Meteorological wind speed and direction measured at four stations within our study area were obtained from the National Data Buoy Center (NDBC) (https://www.ndbc.noaa.gov/ accessed January 2020) (Figure 1b). The measurements were recorded at regular intervals, but the frequency of measurement varied among sites (AMAA2, 30 min; ALIA2, KGCA2, and SNDA2, 6 min). The years represented at each site varied due to instrument installation and operability (see Section 3). For comparison to geographic distribution of age-0 juveniles, we used data from the three years that also had age-0 data (Table 2). For comparison to recruitment, we used all years with data from April to September, note that the years with data varied among the four stations (Table 2).

The available empirical measurements were used to calculate vector components. The components, u (+u = toward the east, a "westerly" wind) and v (+v = toward the north, a "southerly" wind), indicate direction to which the wind was blowing (m/s, degrees clockwise from true North). For a detailed examination of the wind field by site and year, we computed the cumulative sums of each vector beginning on April 1 and progressing cumulatively to October 1; this time period was assumed to be most relevant to displacement of eggs, larvae, and age-0 juveniles. The original units, m/s, were converted to km. Conceptually, the converted and cumulatively summed vectors can be thought of as a progression through time of the hypothetical displacement from a station during any given year and are similar to the progressive wind diagrams of Schlaefer et al. (2018). For relating to recruitment, which required a simpler metric, each component was averaged by three time periods corresponding to when eggs and early larvae are most abundant (April–May), when late larvae and age-0 juveniles are abundant (June–September), and the overall period (April–September).

As a driver of coastal ocean circulation, any surface wind effect on fish distribution may be better understood by considering the hydrographic response. This is especially important in our study area where downwelling may favor nearshore retention of larvae and reduce their southwestward transport as opposed to upwelling-related offshore transport and possible rapid southwestward advection (Bailey et al., 1999; Stabeno et al., 1996). The expectation was for downwelling winds to steepen shoreward-sloping isohalines by decreasing the offshore extent of lower-salinity surface water. Winds favoring upwelling would disperse lower-salinity water offshore. This would be reflected in both surface salinity and isohaline depth. We, therefore, mapped both variables using salinity profiles recorded at each site during EcoFOCI spring and late-summer surveys. At each EcoFOCI survey site (Figure 1b), salinity profiles were measured with a Sea-Bird Electronics 49 Fastcat mounted on the tow wire immediately above the bongo net. The accuracy of the profiler was verified by comparison to data collected periodically

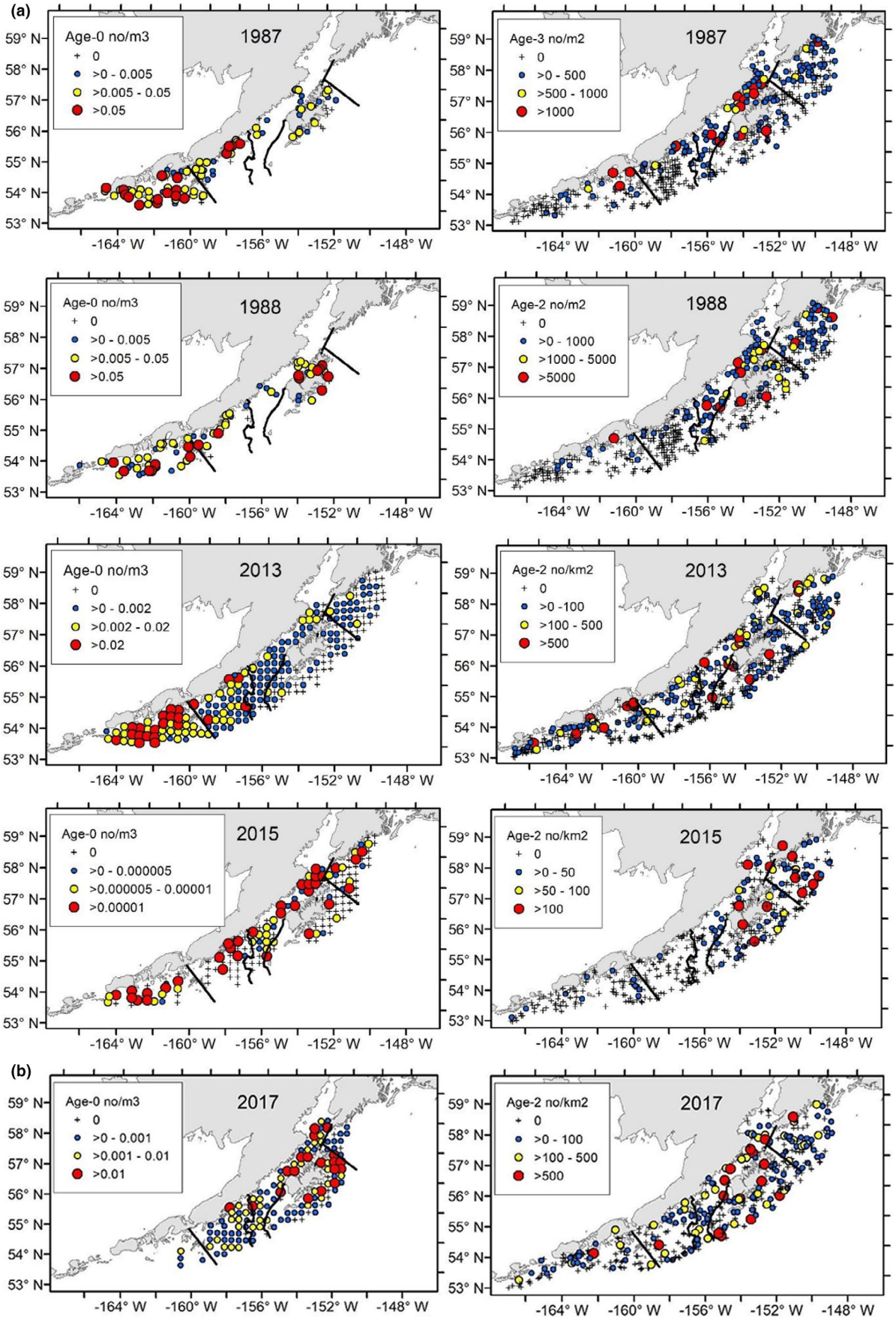

FIGURE 2 Geographic distribution of abundance indices for five walleye pollock cohorts (1987, 1988, 2013, 2015, and 2017) in the western Gulf of Alaska as age-0 juveniles (left panels) and subadults (right panels). Note the difference in symbol size and color scale [Colour figure can be viewed at wileyonlinelibrary.com]

with a Sea-Bird 911 + CTD. Salinity measurements at 1-m-depth intervals during upcasts were used to compute surface salinity and depth of the 32-salinity isohaline. Surface salinity was the integrated mean for the upper 5 m. For isohaline depth, we chose the 32-salinity isohaline because it is intermediate in the range of previously observed coastal salinities within the study area (Reed, Schumacher, & Incze, 1987; Schumacher & Reed, 1980, 1986; Stabeno et al., 2004). These were mapped across sites to provide a spatially comprehensive evaluation of downwelling/upwelling conditions over the area covered during each EcoFOCI spring and late-summer survey. A complementary analysis using data from 50 sites that were commonly sampled each survey was conducted to allow a spatially controlled comparison among years.

2.4 | Recruitment

We tested the relationship between recruitment and surface wind or region-specific age-0 abundance using least-squares linear regression. The recruitment index is an estimate of Gulf-wide abundance at age-1 from the stock assessment (Dorn et al., 2018). The recruitment time series extends from 1970 (1969 year class) to present and is updated annually. For the relationships, we matched recruitment to surface wind or age-0 abundance by year (Table 2). The regression analysis was implemented and evaluated in R (version 3.6.1; R Core Team, 2019) using the *lm* and *anova* functions.

For the surface wind–recruitment relationship, multiple regression was necessary because the predictor variables were wind vectors:

$$M_{y+1}^{0.25} = b_0 + b_1 v_y + b_2 u_y + b_3 v_y u_y + \varepsilon,$$

where $M^{0.25}{}_{y+1}$ denotes 4th-root-transformed recruitment (millions of fish) in year $y+1$, and v_y and u_y denote mean wind vector components in the north–south and east–west directions, respectively, averaged by time period during year y. The term, $v_y u_y$, allows for interaction between the components (e.g., northeast direction). Separate regressions were performed for each of the four NDBC locations described above and for each time period: (1) April–May corresponding to the egg and early-larva stages, (2) June–September corresponding to the late-larva and age-0 juvenile stages, and (3) overall April–September. Abundance estimates were 4th-root-transformed as needed to ensure that error (ε) was normally distributed.

For the age-0 abundance–recruitment relationship, multiple regression was necessary to include a region effect:

$$M_{y+1} = b_0 + b_1 D_{yr} + b_2 \text{Region} + b_3 D_{yr} \text{Region} + \varepsilon,$$

where M_{y+1} denotes Gulf-wide recruitment (millions of fish) in year $y+1$ and D_{yr} is the 4th-root-transformed mean population density of age-0 juveniles in year y (1987, 1988, 2013, 2015, and 2017) by *Region r* (Kodiak, Shelikof, Semidi, and SW). The 4th-root-transformation of age-0 densities, but not recruitment, linearized the relationship and gave a more normal error (ε) structure. A power analysis was conducted if the interaction (D_{yr}Region) was not significant ($p > .05$) (Shieh, 2019).

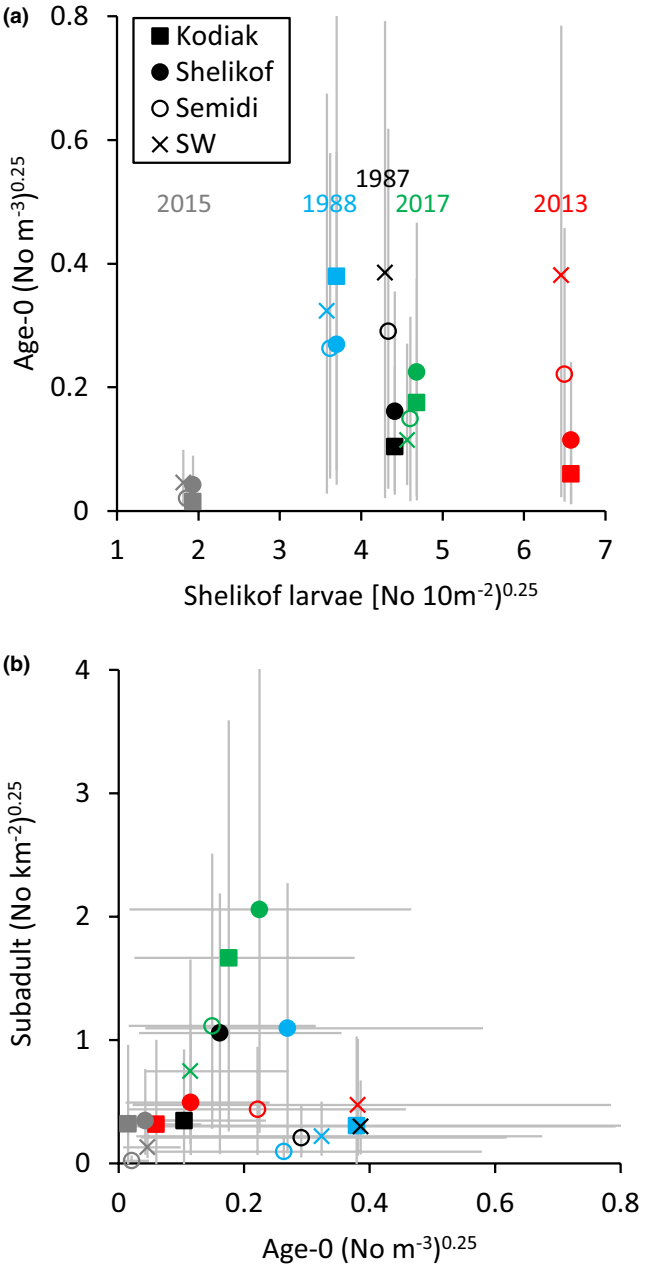

FIGURE 3 Region- and year-specific mean (± *SE*) population density of age-0 juvenile walleye pollock during late summer in relation to (a) population density of Shelikof larvae (points are offset to show error bars) and (b) to region- and year-specific mean population density of subadult walleye pollock [Colour figure can be viewed at wileyonlinelibrary.com]

3 | RESULTS

3.1 | Fish distribution

Considerable variation was evident in the geographic distribution of population density among the five-year classes (Figure 2). The

TABLE 3 Analysis of variance of mean population density of age-0 walleye pollock ((number m^{-3})$^{0.25}$) by region for five-year classes with annual mean population density ((number 10 m^{-2})$^{0.25}$) of Shelikof larvae as a covariate. Power of slope heterogeneity test = 0.05

	Sum Sq	*df*	*F* value	Pr(>*F*)
Intercept	0.011	1	0.653	0.435
larvae	0.034	1	2.035	0.179
Region	0.010	3	0.194	0.898
larvae:Region	0.027	3	0.539	0.665
Residuals	0.200	12		

TABLE 4 Analysis of variance of the relationship between mean population density of subadult (age 2 or 3, see text) (number km^{-2})$^{0.25}$ and age-0 (number m^{-3})$^{0.25}$ walleye pollock by region for five-year classes. Power of slope heterogeneity test = 0.21

	Sum Sq	*df*	*F* value	Pr(>*F*)
Intercept	0.623	1	2.287	0.156
age-0	0.449	1	1.649	0.223
Region	0.121	3	0.149	0.929
age-0:Region	0.861	3	1.053	0.405
Residuals	3.268	12		

1987 and 2013 year classes were most abundant in southwestern regions as age-0 juveniles; as subadults, population density was more evenly distributed across the study area. The 1988 and 2015 year classes were widespread as age-0 juveniles and most abundant in northeastern regions as subadults; the 2015 year class was much lower in abundance than all other year classes. The 2017 year class was most abundant in northeastern regions as both age-0 and subadults.

Overall, the highest regional population density of age-0 juveniles occurred in the SW region. High density corresponded with high abundance of larvae upstream in the Shelikof core area (Figure 3a). While consistent with downstream drift, the downstream increase in age-0 juvenile abundance was not evident for all year classes suggesting a year–region interaction. The interaction term in the least-squares multiple linear regression was not significant ($F = 0.539$, $p = .665$) (Table 3); however, power of the slopes heterogeneity test indicated only a 0.05 probability (beta = 0.95) of a significant outcome if the real difference was equal to the minimum effect size.

High population density of age-0 juveniles did not translate into high density of subadults in downstream regions (Figure 3b). However, the test of year–region interaction ($F = 1.05$, $p = .405$) (Table 4) again suffered from low power of the slopes heterogeneity test (power = 0.21). Interestingly, highest densities of subadults corresponded with intermediate densities of Shelikof larvae and age-0 juveniles in the Shelikof and Kodiak regions.

3.2 | Wind and salinity

Interannual differences in the progression of surface wind speed and direction from April through September were evident at each of the four NDBC sites despite an apparent site effect (Figure 4). At SNDA2, the cumulative-vector trajectory, or hypothetical displacement, was initially southward before turning eastward. The initial southward displacement was greatest in 2013 and least in 2015. At AMAA2, the trajectory in 2013 was southward and then eastward, whereas in 2015, it was westward, then northward, and finally eastward. The 2017 trajectory was intermediate. The strong northerly wind event noted at AMAA2 on September 19–24, 2013, coincides with the gap-wind event detailed by Ladd, Cheng, and Salo (2016) and is discussed later. At KGCA2, southeastward wind prevailed in all years but the hypothetical displacement from April 1 to commencement of the spring survey was furthest during 2013. At ALIA2, the year-specific trajectories were similar to those at AMAA2. These trajectories indicate that surface wind conditions were quite different between 2013 and 2015 with intermediate conditions during 2017. This contrasts somewhat with the geographic distributions of age-0 juveniles, which indicate that 2013 (highest abundance southwest) and 2017 (highest abundance northeast) were quite different while 2015 (more or less evenly distributed, but very low abundance) was intermediate. Although wind conditions in 2017 appeared intermediate, the salinity signal was not.

Surface salinity and depth of the 32-salinity isohaline varied geographically in accordance with known ACC influence, but with considerable variation among years. Surface salinity and isohaline depth (Figures 5 and 6) were low and deep, respectively, along the Alaska and Kenai peninsulas consistent with the expected location of relatively fresh ACC water. Higher surface salinity and shallower isohaline depth were observed over the shelf along the Gulf-side (as opposed to the Shelikof side) of Kodiak Island that typically receives relatively little ACC water. A spatially controlled comparison among years was made using data from sites that were commonly sampled each survey. At these sites ($n = 50$), interannual differences in surface salinity and isohaline depth were evident despite an apparent increase in freshwater influence from spring to late summer (Table 5). During 2013, surface salinity and isohaline depth were, on average, intermediate between 2015 and 2017. During 2015, mean surface salinity and isohaline depth were low and deep, respectively, indicating relatively high freshwater influence that was associated with northward (AMAA2, ALIA2) and reduced southward (SNDA2, KGCA2) surface wind. During 2017, spring and late summer, mean surface salinity and isohaline depth were high and shallow (Table 5), respectively, indicating relatively low freshwater buildup within the study area. Importantly, the confinement of lower-salinity water in 2017 to along the Alaska Peninsula and over the southern Shelikof sea valley (Figures 5 and 6) was consistent with downwelling.

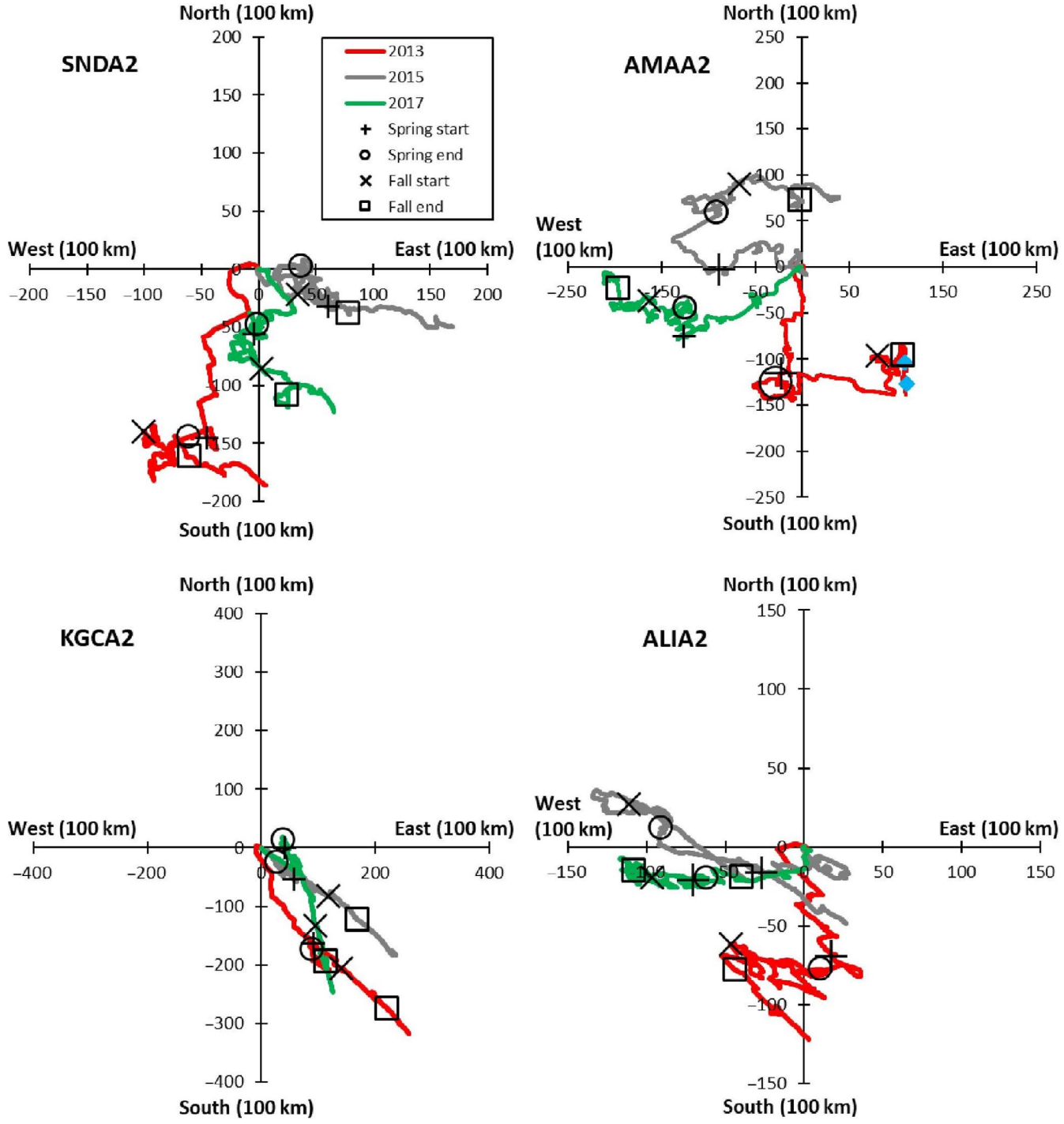

FIGURE 4 Progressive wind diagrams at four NDBC stations (Figure 1): SNDA2, AMAA2, KGCA2, and ALIA2 for April–September 2013, 2015, and 2017. Black symbols indicate start and end dates of EcoFOCI spring and late-summer surveys. Blue diamonds indicate September 19 and 24, 2013 (AMAA2 only) [Colour figure can be viewed at wileyonlinelibrary.com]

3.3 | Recruitment

The relationship between wind, region-specific age-0 juvenile abundance, and recruitment could not be fully tested because wind and age-0 abundance were both available for only three years; however, the wind–recruitment and age-0 abundance–recruitment relationships were significant. Data availability required each relationship to be evaluated using different year-class groups.

Significance of the wind–recruitment relationship was dependent on NDBC site. At AMAA2, located just upstream of the Shelikof spawning area, sufficient wind data were available for 12 years and 84% of the variation in walleye pollock recruitment was explained by April–May mean surface wind (p = .001, Table 6). Interaction between the u and v components was significant (p = .011, Table S1). Recruitment increased as the mean wind became increasingly southwestward (Figure 7). At other NDBC sites, the available wind time

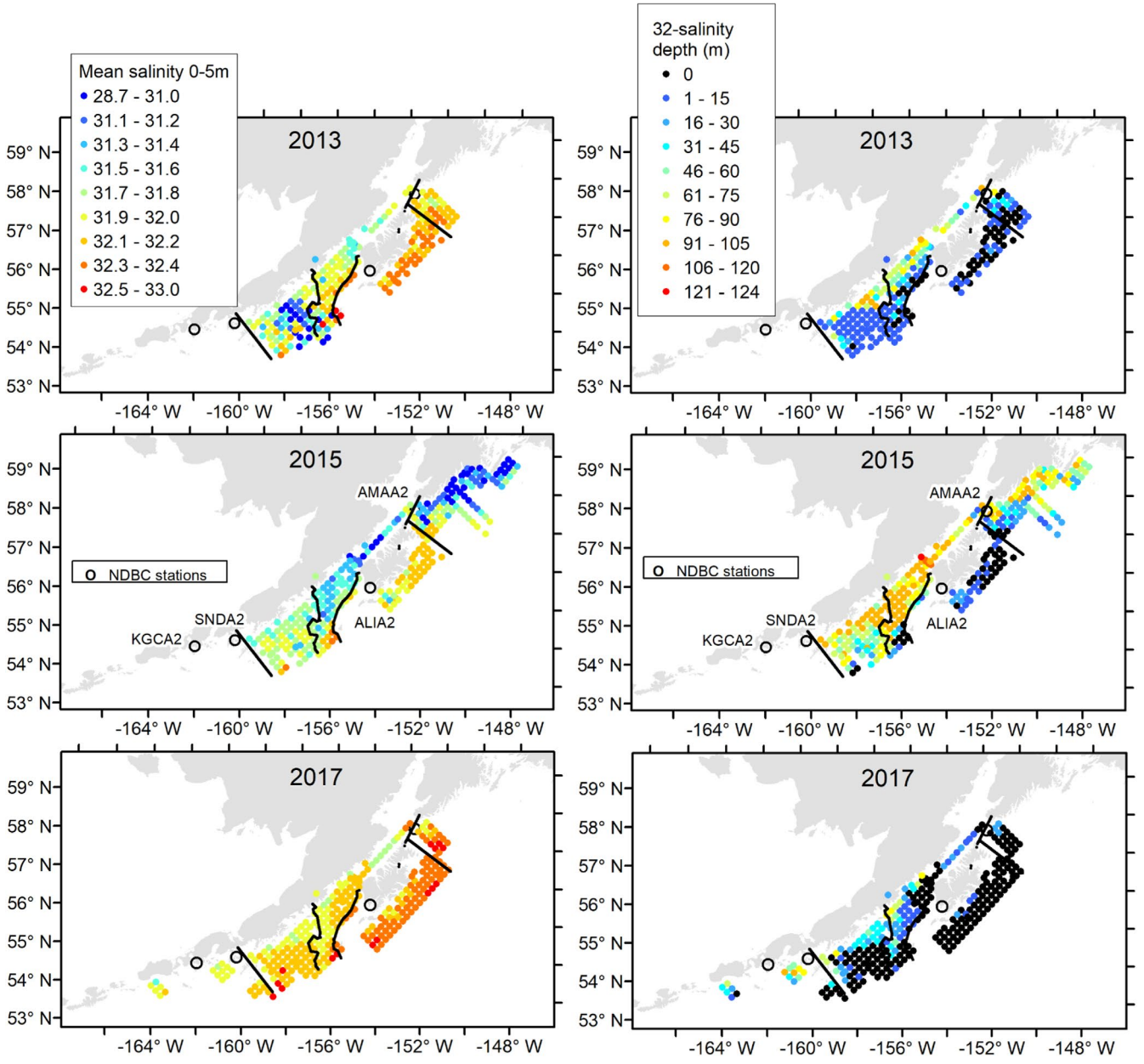

FIGURE 5 Mean surface salinity (0–5 m depth) (left panels) and depth of the 32-salinity isohaline (right panels) at EcoFOCI sites in the western Gulf of Alaska during May–June 2013, 2015, and 2017 [Colour figure can be viewed at wileyonlinelibrary.com]

series were only 7–8 years. At KGCA2, 96% and 90% of the variation in recruitment was explained by wind vectors averaged for April–September ($p = .014$) and April–May ($p = .049$), respectively (Table 6). The *u*-*v* interaction term was significant ($p = .007$, Table S1) for the April–September period, but no regression coefficients were significant for the April–May period for which the regression was only marginally significant. Recruitment increased as the mean wind became increasingly southeastward; we note that there were few points with intermediate recruitment (Figure 7). No other wind–recruitment relationships were significant (Table 6). Interestingly, the mean wind vectors at AMAA2 and KGCA2 were related (AMAA2, April–May; KGCA2, April–September; $n = 7$, 2009–2015); Pearson correlation was −0.65 and 0.74 for the *u* and *v* components, respectively. The negative correlation for *u* indicates that westward wind at AMAA2 generally corresponded with an eastward wind at KGCA2.

Significance of the relationship between mean age-0 population density and recruitment was dependent on region. Among the five-year classes with age-0 distribution data, 96% and 88% of the variation in walleye pollock recruitment was explained by the population density of age-0 juveniles in the Kodiak and Shelikof regions, respectively. The relationships were significant ($p < .05$) (Table 7), and regression slopes were positive (Figure 8). In contrast, age-0 abundance in the Semidi or SW regions was not significantly related to recruitment ($p > .05$). A more rigorous analysis would be to test for slope heterogeneity among regions; however, we had low confidence in accepting the hypothesis of no difference because the power of test = 0.22.

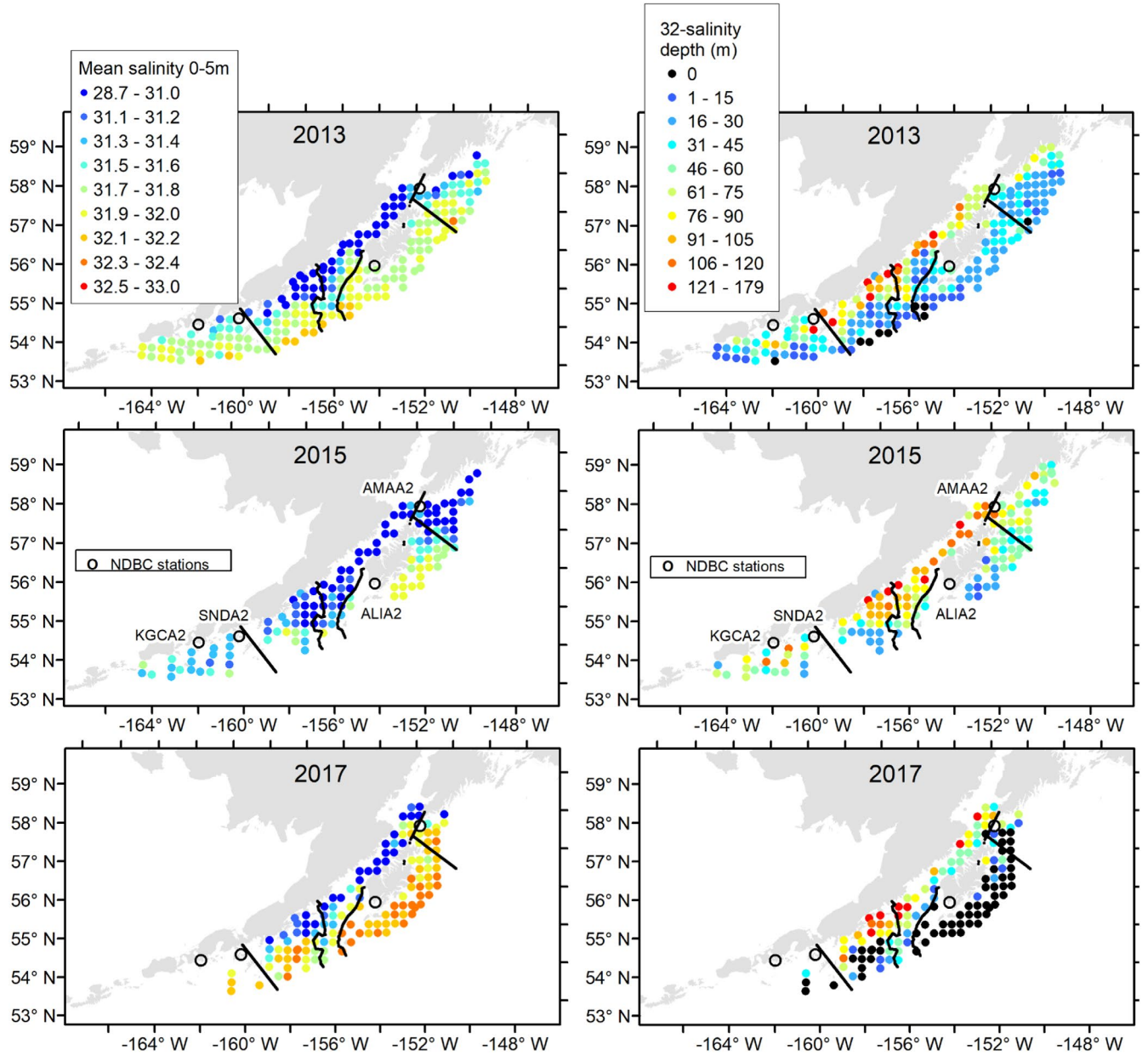

FIGURE 6 Mean surface salinity (0–5 m depth) (left panels) and depth of the 32-salinity isohaline (right panels) at EcoFOCI sites in the western Gulf of Alaska during August–September 2013, 2015, and 2017 [Colour figure can be viewed at wileyonlinelibrary.com]

Nevertheless, the significant dependence of recruitment on downwelling-favorable northeasterly wind into Shelikof Strait (at AMAA2) and on age-0 juvenile abundance in the Kodiak and Shelikof regions indicates that wind-related retention of early life stages in these areas can reasonably be considered a determinant of year-class strength.

4 | DISCUSSION

Our results indicate that high population densities of age-0 juveniles in the Shumagin and SW regions can be explained by downstream drift of eggs, larvae, and juveniles from the Shelikof spawning area, that the high downstream densities are unlikely to contribute proportionally to recruitment in the GOA, and that wind-driven transport from higher-quality rearing habitat upstream adversely affects recruitment. We hypothesize that springtime (April–May) surface wind is a determinant of whether larvae are retained in upstream nurseries of superior habitat quality that favor recruitment. We first provide prerequisite evidence of geographic variation in habitat suitability before discussing why wind-driven transport is key to the most parsimonious explanation for the observed interannual variation in age-0 geographic distribution and recruitment.

We consider retention to be a criterion of suitability for habitat that supports potential recruits. A large-scale model indicated that proximity of source areas to the western exit of the GOA, Unimak Pass, increased propagule export to the Bering Sea (Parada

TABLE 5 Mean and standard error (*SE*) of (1) surface salinity and (2) depth of the 32-salinity isohaline at the same 50 sites sampled during each EcoFOCI cruise in the western Gulf of Alaska during spring and late-summer 2013, 2015, and 2017

Variable	EcoFOCI cruise	Year	Mean	*SE*
Surface salinity	Spring	2013	31.76	0.093
		2015	31.66	0.050
		2017	32.07	0.027
	Late summer	2013	31.23	0.110
		2015	31.16	0.085
		2017	31.73	0.072
32-salinity isohaline depth (m)	Spring	2013	22.10	4.437
		2015	51.09	5.762
		2017	10.95	2.659
	Late summer	2013	46.83	4.359
		2015	61.72	4.562
		2017	37.26	5.978

et al., 2016). We acknowledge that exports might return to their natal stock. While we cannot yet conclusively differentiate the export and mortality vectors of loss, regional differences in juvenile walleye pollock demographics indicate that the Kodiak and Shelikof regions provide greater food-related benefits than other regions downstream. The benefits relate to influxes of oceanic water and high densities of large krill (*Thysanoessa* spp.), which are preferred, energy-rich prey of juvenile walleye pollock (Mazur, Wilson, Dougherty, Buchheister, & Beauchamp, 2007; Wilson, Buchheister, & Jump, 2011; Wilson et al., 2013). Juveniles in the Kodiak vicinity are larger (Wilson, 2000) and better provisioned than their downstream counterparts for the onset of winter (Buchheister et al., 2006). Exchange between juveniles in these regions and their downstream counterparts becomes constrained by late summer (Wilson et al., 2018) or possibly earlier based on model-based estimates of retention in the Kodiak region (Hinckley et al., 2001). With the onset of winter, age-1 juveniles likely concentrate locally in deep areas such as sea valleys (Brodeur & Wilson, 1996; Wilson, 2009). While we did not focus on evaluating the potential for negative density dependence, it is noteworthy that in the Shelikof and Kodiak regions intermediate densities of age-0 juveniles resulted in the highest population densities of subadults, and that the age-0 juvenile–recruitment relationship appeared to be nonlinear (only age-0 density was 4th-root-transformed). There is potential for density dependence among GOA walleye pollock due to prey shortage resulting from intraspecific competition (Duffy-Anderson, Bailey, & Ciannelli, 2002), interspecific competition, or temperature-related increase in metabolic demand (Ciannelli, Chan, Bailey, & Stenseth, 2004). Nevertheless, we attribute the superior forecast performance of the Kodiak and Shelikof regions to high habitat suitability, including apparent retention mechanism(s), and to interannual variation in propagule delivery, which likely depends at least partly on wind-driven transport.

Oceanographically, the western coastal GOA is characterized as a downwelling system with intermittent upwelling. During winter, cyclonic winds drive downwelling along the coast. These winds weaken during summer, and upwelling-favorable northerly and westerly winds are common (Ladd, Stabeno, & Cokelet, 2005; Stabeno et al., 2004). We used maps of surface salinity and the 32-salinity isohaline depth as supplemental indicators of upwelling–downwelling conditions because downwelling traps fresher, buoyant water along the coast while upwelling spreads it offshore (Rogers-Cotrone et al., 2008). In the California Current System, periodic upwelling exposes propagules to alongshore flow over the shelf and is believed to be an evolutionary driver of spawn timing and larval duration (Shanks & Eckert, 2005). Pollock spawn timing in Shelikof Strait puts larvae and early juveniles in the water column during spring and summer when 52-year mean winds are weakly downwelling (Ladd et al., 2005; Stabeno et al., 2004), and wind-driven transport encompasses its annual low (Stabeno et al., 2016). We focus on wind-related transport because larval walleye pollock are weak swimmers with little ability to control their horizontal distribution (Davis, 2001), and there are no data for these year classes to comparatively assess how larval vertical position might have indirectly affected transport. To gain insight on possible underlying mechanisms, we focus on the three years that had wind, salinity, and extensive fish distribution data: 2013, 2015, and 2017.

During 2013, sustained northerly and westerly winds during spring and summer, respectively, and subsurface depth of the 32-salinity isohaline over much of the study area were associated with high age-0 abundance downstream, in the SW Region. Northerly winds blow offshore while westerlies would be slightly upwelling (Stabeno et al., 2004). Furthermore, orographic features on the Alaska Peninsula can intensify the wind effect on oceanography. For example, a northerly wind event during September 19–24, 2013, was intensified as it blew southward through orographic gaps toward northeast Kodiak Island. The oceanographic response was profound; the gap-wind event diverted ACC flow away from Shelikof Strait and around the outside of Kodiak Island (Ladd et al., 2016). Gap winds can be large-scale events affecting ocean conditions from the coast to ~150 km beyond the shelf for days to weeks. Interestingly, such events have become increasingly common from 1999 to 2009 with strong offshore wind days inversely related to Pacific/North American and Pacific Decadal Oscillation indices (Ladd et al., 2016). For context, we annotated the progressive wind diagram for NDBC site AMAA2 to indicate the occurrence of this specific gap-wind event. We note the similarity on the diagram in direction of winds during this gap-wind event to winds earlier during spring (April–May). The implication is that strong northerly wind during spring caused substantial offshore diversion of coastal water away from retention areas along the coast and was then transported southwestward possibly in the Alaskan Stream (Ladd et al., 2016). This is consistent with the observed large area of <32-salinity surface water. Downstream transport from Shelikof Strait to the SW region (~550 km) over the 77 days until the late-summer survey is conceivable given

TABLE 6 Analysis of variance of walleye pollock recruitment (millions$^{0.25}$) in relation to annual mean surface wind vector components (*u*, *v*) at each of four National Data Buoy Center sites (AMAA2, KGCA2, SNDA2, and ALIA2) and three time periods (April–September, April–May, June–September).

NDBC site	Period	Term	Sum Sq	*df*	*F*	Pr(>*F*)	R^2
AMAA2	April–September	Regression	35.57	3	1.236	0.359	.32
		Residuals	76.74	8			
		Total	112.30	11			
	April–May	Regression	94.48	3	14.133	**0.001**	.84
		Residuals	17.83	8			
		Total	112.30	11			
	June–September	Regression	25.68	3	0.790	0.532	.23
		Residuals	86.63	8			
		Total	112.30	11			
KGCA2	April–September	Regression	96.35	3	22.797	**0.014**	.96
		Residuals	4.23	3			
		Total	100.57	6			
	April–May	Regression	90.87	3	9.366	**0.049**	.90
		Residuals	9.70	3			
		Total	100.57	6			
	June–September	Regression	32.29	3	0.473	0.723	.32
		Residuals	68.28	3			
		Total	100.57	6			
SNDA2	April–September	Regression	68.25	3	5.315	0.070	.80
		Residuals	17.12	4			
		Total	85.37	7			
	April–May	Regression	59.45	3	3.058	0.154	.70
		Residuals	25.92	4			
		Total	85.37	7			
	June–September	Regression	5.83	3	0.098	0.957	.07
		Residuals	79.54	4			
		Total	85.37	7			
ALIA2	April–September	Regression	8.85	3	0.096	0.957	.09
		Residuals	91.83	3			
		Total	100.68	6			
	April–May	Regression	64.36	3	1.772	0.325	.64
		Residuals	36.32	3			
		Total	100.68	6			
	June–September	Regression	37.45	3	0.592	0.661	.37
		Residuals	63.23	3			
		Total	100.68	6			

Note: A separate analysis was conducted for each NDBC site and time period.
Bold font indicates statistical significance (*p*-values < .05).

reasonable drift speeds (5–10 cm/s) (Hinckley et al., 2001; Parada et al., 2016). The very similar distribution of age-0 juveniles during 1987 was caused by downstream transport as demonstrated by five successive surveys from spring through summer and satellite-tracked buoys (Hinckley et al., 1991).

Alternatively, the SW age-0 juveniles in 2013 might have been spawned in the Shumagin sea valley where spawning occurs ~1 month earlier than in Shelikof. Unfortunately, hatchdate estimates for the 2013 year class are not available (A. Dougherty pers. communication), but fish with hatchdates corresponding to the earlier spawn timing have never been found in the GOA (Dougherty, Bailey, & Mier, 2007; Dougherty, Bailey, Vance, & Cheng, 2012) possibly because they are exported from the system (Parada et al., 2016). For both the 1987 and 2013 year classes, the high abundance of age-0

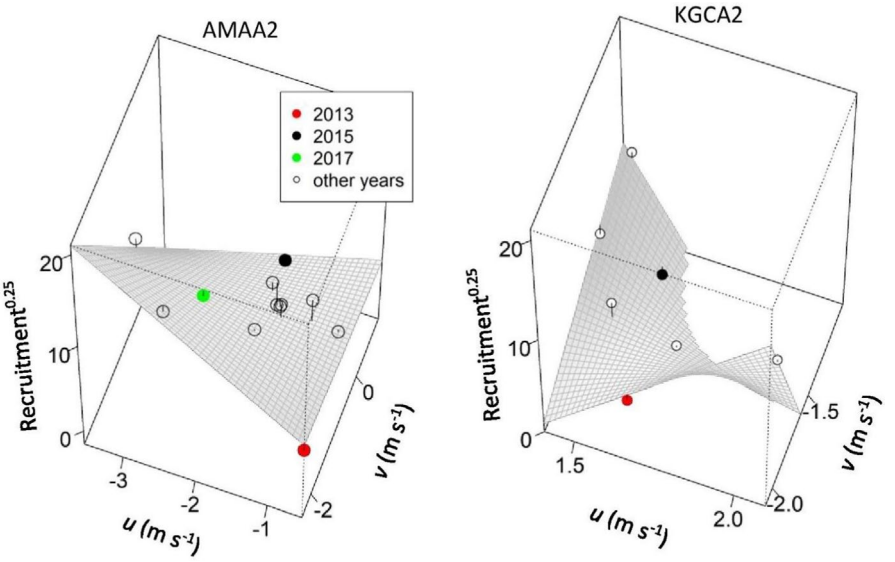

FIGURE 7 Gulf-wide recruitment of walleye pollock ($M^{0.25}$) in relation to mean *u* and *v* wind vector components (ms^{-1}) at NDBC locations AMAA2 during April–May (left panel), and KGCA2 during April–September (right panel). The shaded mesh surface represents the least-squares multiple linear regression. Note, *u* and *v* axes differ between plots [Colour figure can be viewed at wileyonlinelibrary.com]

TABLE 7 Analysis of variance of walleye pollock recruitment (millions) in relation to the population density at age 0 ($(no\ m^{-3})^{0.25}$) separately for each of four regions (Kodiak, Shelikof, Semidi, and SW).

Region	Term	Sum Sq	*df*	*F*	Pr(>*F*)	R^2
Kodiak	Regression	72,434,476	1	70.945	**0.004**	.96
	Residuals	3,063,005	3			
	Total	75,497,481	4			
Shelikof	Regression	66,476,718	1	22.108	**0.018**	.88
	Residuals	9,020,763	3			
	Total	75,497,481	4			
Semidi	Regression	31,125,949	1	2.104	0.243	.41
	Residuals	44,371,532	3			
	Total	75,497,481	4			
SW	Regression	10,895,156	1	0.506	0.528	.14
	Residuals	64,602,326	3			
	Total	75,497,481	4			

Bold font indicates statistical significance (*p*-values < .05).

juveniles downstream is therefore most parsimoniously explained by downstream transport of propagules originating mostly from the Shelikof spawning area.

During 2015, the northerly wind component was reduced and the large areal extent of the deep surface layer of ≤32-salinity water was associated with a relatively even geographic distribution of age-0 juvenile abundance, which was remarkably low. The unprecedented low abundance of Shelikof larvae and age-0 juveniles presumably reflects very high mortality prior to the EcoFOCI spring survey (Rogers et al., 2020). Proposed mechanisms include eggs sinking in the low-salinity water to the seafloor where pelagic egg survival may be low, and density-dependent mortality of larvae insufficiently dispersed by the anomalously low-flow environment (Rogers et al., 2020). Compared to other years, the relaxation of northerly wind might have reduced southward transport causing a buildup of low-salinity surface water, but anomalously high temperatures might also have elevated freshwater inputs (Batten et al., 2018; Rogers et al., 2020). Interestingly, the southernmost part of the Shelikof Region where we observed higher-salinity water throughout the water column was approximately where larval densities were relatively high (Dougherty et al., 2019). If the mortality of Shelikof larvae was higher than the mortality of progeny spawned elsewhere, it could explain the evenness in distribution of age-0 abundance; however, we have no evidence of spatial variation in larval mortality. Later, at age 2, during summer 2017, the relatively high abundance of subadults in northeastern regions is consistent with habitat more favorable for growth and survival than downstream habitat; admittedly, we cannot distinguish higher survival from directed southwest-to-northeast movement of this year class of juveniles after September 2015.

During 2017, northeasterly wind at the two easternmost NDBC sites and confinement of <32-salinity surface water to the inner and middle shelf, indicative of downwelling, were associated with high age-0 population densities in the Shelikof and Kodiak regions. Conditions in 2017 appear to have been similar to 1988 when model-based northeasterly wind in Shelikof Strait occurred during

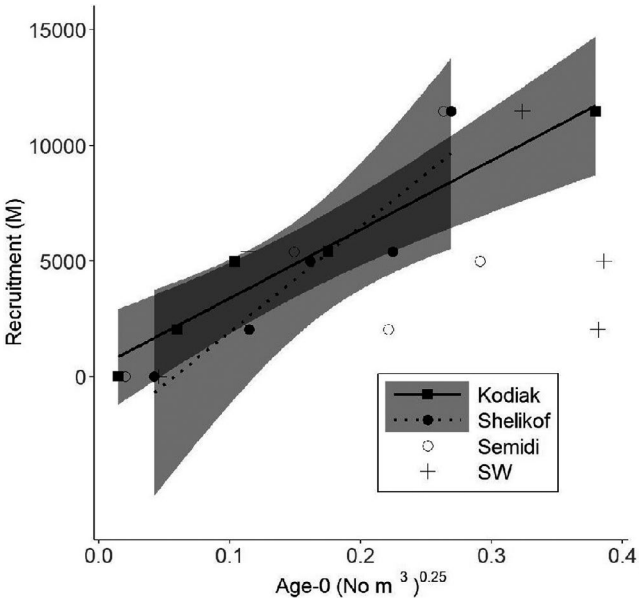

FIGURE 8 Gulf-wide recruitment of walleye pollock (millions) in relation to population density of age-0 juvenile walleye pollock in each of four regions in the Gulf of Alaska during late-summer 1987, 1988, 2013, 2015, and 2017. Lines (with 95% confidence intervals) represent significant least-squares linear regression (i.e., regressions for Semidi and SW regions were not significant)

January–May (Hermann, Hinckley, Megrey, & Stabeno, 1996) with notable weakening in late April 1988; in fact, Bailey and Macklin (1994) attribute the strong 1988 year class to protracted calm during spring 1988, similar to the wind pattern in 2017.

The enduring relevance of wind to GOA walleye pollock recruitment is demonstrated by its explanation of significant variance over long time series (1961–1995) (Lee et al., 2009) and over our more recent study period. We focus here on the direct mechanisms of turbulent mixing and transport (Chan, Zhang, & Bailey, 2010), but recognize that possible wind effects on primary production and zooplankton are also relevant to walleye pollock recruitment. First, wind-driven turbulence was associated with low survival of larvae (Bailey & Macklin, 1994). The proposed mechanism is that larvae avoid high turbulence (Davis, 2001) and experience reduced feeding success under low-light conditions (Porter et al., 2005) such as occur at depth below turbulent surface layers. This was considered more likely than an inverse turbulence-sea surface temperature effect (Ciannelli et al., 2004). Second, transport in the western GOA is driven by northeasterly wind along the coast where topographic and mesoscale features enhance retention (Stabeno et al., 1996). This can explain our observation that increasingly northeasterly wind upstream of the main spawning area (AMAA2) when eggs and larvae are most abundant (April–May) resulted in higher recruitment. Future application of this relationship (e.g., recruitment forecast) can be simplified by rotating the axes 40 degrees counterclockwise to approximate alignment of the *u*-axis with Shelikof Strait; preliminarily, this eliminated significant *u-v* interaction indicating that wind speed in the along-Strait (NE-SW) direction is most relevant to recruitment. We suspect that the location and timing of wind is important and attribute the significant wind–recruitment farther downstream, at KGCA2, to fewer years of data when recruitment was intermediate and to the AMAA2-KGCA2 correlation in wind vectors. It is not yet clear how the wind at AMAA2 relates to the smaller-scale circulation dynamics that affect the dispersion and advection of eggs and larvae (e.g., Incze et al., 1989). Smaller-scale dynamics, however, likely determine whether larvae are retained or transported offshore where slow growth and rapid southwestward advection might lower the probability of recruitment to the GOA stock (Bailey et al., 1995; Hinckley et al., 1993). Biophysical modeling identified likely retention-nursery areas along the coast and around Kodiak Island while export of larvae and age-0 juveniles to the Bering Sea represents loss from the GOA (Parada et al., 2016). Previous models of walleye pollock recruitment in the GOA account for wind speed as a determinant of turbulence (Ciannelli et al., 2005; Lee et al., 2009; Megrey, Hollowed, Hare, Macklin, & Stabeno, 1996) while the relevance of wind direction has been overlooked despite conceptual (Bailey et al., 2005), model-based (Parada et al., 2016), and empirical support. We believe that resolving the effect of wind on small-scale circulation that affects egg and larval dispersal and advection from the Shelikof core area is key to understanding subsequent age-0 juvenile distributions that together with information on habitat quality will help solve the recruitment puzzle.

The direction of wind-driven transport is relevant to recruitment in other systems. On the Great Barrier Reef over 23 years, wind direction was a significant factor in strong recruitment events of snapper (*Lutjanus carponotatus*) (Schlaefer et al., 2018). For cod (*Gadus morhua*), retention of eggs in a Newfoundland fjord was related to wind direction and speed (Knickle & Rose, 2010) while retention of larvae along the Norwegian coast was explained by downwelling-favorable southwesterly wind, which is common during positive phases of the North Atlantic Oscillation (Endo et al., 2020). In the Bering Sea, wind-driven transport direction of walleye pollock early life stages varied with climate phases and is hypothesized to affect spatial overlap of juveniles and adults thereby affecting cannibalism (Wespestad, Fritz, Ingraham, & Megrey, 2000). There is support for predation of juveniles controlling GOA walleye pollock recruitment (Bailey, 2000; Zhang, Bailey, & Chan, 2010) and more study is needed to determine whether the spatial dynamics (e.g., predator–prey spatial overlap) relate to transport. These studies underscore wind as a significant density-independent (activating) factor in the stochasticity of recruitment (Bailey et al., 2005; Houde, 2008) and population connectivity (Cowen, Gawarkiewicz, Pineda, Thorrold, & Werner, 2007).

Some caveats should be considered when evaluating our results. First, age-0 sampling methods differed between the RACE and EcoFOCI surveys. The expectation of targeting echosign during the RACE surveys likely introduced an upward bias by reducing effort devoid of echosign (Wilson, 2000; Wilson, Brodeur, & Hinckley, 1996). This may have elevated our estimates of age-0 density for these two years with consequent effects on regression parameters. Second, subadult walleye pollock occur throughout the water column so that only a portion of the population is sampled by trawling

on the seafloor. It is unknown whether this biases estimates of geographic distribution of population density. Shima, Hollowed, and Van Blaricom (2002) also used RACE bottom-trawl data to infer age-specific distribution patterns of walleye pollock. Their length-at-age category for age-2 fish (230–330 mm) was based on all summertime historical length data. Direct comparison with their results is difficult because their region-specific estimates for age-2 fish focused on the proportion of stations with low (<1,000 fish km^{-2}) population density. Third, we interpreted surface salinity and the depth of the 32-salinity isohaline, together with wind displacement, to characterize flow; however, we did not account for possible interannual differences in freshwater inputs. This is a potentially important omission as freshwater input is an important determinant of salinity over the shelf. Nevertheless, we believe the observed patterns in wind displacement, salinity, and fish distribution, when taken together, provide compelling circumstantial evidence of a real response in fish distribution to flow characteristics. Fourth, we acknowledge that our five focal year classes (1987, 1988, 2013, 2015, and 2017) straddle the well-studied 1988/1989 regime shift (Litzow et al., 2019) and the 2014–2016 warm anomaly (Bond, Cronin, Freeland, & Mantua, 2015). However, our data were insufficient for a before–after analysis of potential climate-related effects; therefore, we focused on the most parsimonious explanation for variation in age-0 distribution that is likely to endure as relevant to recruitment across basin-scale climate variability. Finally, the number of age-1 recruits estimated by the assessment model is updated every year and this will affect the regression statistics.

In summary, there is long-standing recognition that meteorological, hydrodynamical, and biological factors interactively affect recruitment (Houde, 2008; Huse, 2016). We focused here on the cause and consequence of variation in the geographic distribution of age-0 juveniles in the GOA and our findings suggest that wind-driven transport interacts with a spatial mosaic of habitat suitability to affect recruitment. This has fundamental utility as we explore how to integrate transport and retention mechanisms in models of stock dynamics (e.g., Romagnoni et al., 2020). It also has system-level importance because directional alignment between flow and spatial translation of suitable habitat is hypothesized to affect the rate at which populations redistribute geographically (e.g., poleward flowing current aligned with global climate-forced spatial translation of isotherms) (Sorte, 2013). While the GOA ichthyoplankton community is diverse (Doyle et al., 2019), habitat requirements for the juvenile stage of many species are not well known. This is a major shortfall in our understanding of the mechanisms controlling species-specific recruitment, which is critical for anticipating system-wide response to novel climate regimes (Bailey et al., 2005; Litzow et al., 2019).

ACKNOWLEDGEMENTS

We are grateful to L. Rogers for providing the estimates of larva population density in the Shelikof core area, for consultation throughout this project, and for encouraging us to consider the "other years." Discussion early on with S. Kotwicki helped focus this work. Comments by the AFSC Publications Unit personnel, M. Dorn, S. Kotwicki, C. Ladd, L. Rogers, and L. Logerwell improved the manuscript. This research is contribution EcoFOCI-0943 to NOAA's Ecosystems and Fisheries-Oceanography Coordinated Investigations.

CONFLICT OF INTEREST

The authors have no conflict of interest to declare.

AUTHOR CONTRIBUTION

MTW conceived and designed the project, acquired all but the RACE-GAP fish data, analyzed and interpreted the data, and drafted the manuscript. NL acquired the RACE-GAP data, prepared it for analysis, and assisted in revising the manuscript. Both authors give final approval of the version to be published; take public responsibility for its content; and agree to be accountable for all aspects of the work in ensuring that questions related to the accuracy or integrity of any part of the work are appropriately investigated and resolved.

DATA AVAILABILITY STATEMENT

The data that support the findings of this study are available from the corresponding author upon reasonable request.

ORCID


Matthew T. Wilson https://orcid.org/0000-0003-0651-8428

REFERENCES

Bailey, K. M. (2000). Shifting control of recruitment of walleye pollock *Theragra chalcogramma* after a major climatic and ecosystem change. *Marine Ecology Progress Series*, *198*, 215–224. https://doi.org/10.3354/meps198215

Bailey, K. M., Bond, N. A., & Stabeno, P. J. (1999). Anomalous transport of walleye pollock larvae linked to ocean and atmospheric patterns in May 1996. *Fisheries Oceanography*, *8*, 264–273. https://doi.org/10.1046/j.1365-2419.1999.00113.x

Bailey, K. M., Canino, M. F., Napp, J. M., Spring, S. M., & Brown, A. L. (1995). Contrasting years of prey levels, feeding conditions and mortality of larval walleye pollock *Theragra chalcogramma* in the western Gulf of Alaska. *Marine Ecology Progress Series*, *119*, 11–23. https://doi.org/10.3354/meps119011

Bailey, K. M., Ciannelli, L., Bond, N. A., Belgrano, A., & Stenseth, N. C. (2005). Recruitment of walleye pollock in a physically and biologically complex ecosystem: A new perspective. *Progress in Oceanography*, *67*, 24–42. https://doi.org/10.1016/j.pocean.2005.06.001

Bailey, K. M., & Macklin, A. (1994). Analysis of patterns in larval walleye pollock *Theragra chalcogramma* survival and wind mixing events in Shelikof Strait, Gulf of Alaska. *Marine Ecology Progress Series*, *113*, 1–12. https://doi.org/10.3354/meps113001

Bailey, K. M., Zhang, T., Chan, K.-S., Porter, S. M., & Dougherty, A. B. (2012). Near real-time forecasting of recruitment from larval surveys: Application to Alaska pollock. *Marine Ecology Progress Series*, *452*, 205–217. https://doi.org/10.3354/meps09614

Batten, S. D., Raitsos, D. E., Danielson, S., Hopcroft, R., Coyle, K., & McQuatters-Gollop, A. (2018). Interannual variability in lower trophic levels on the Alaskan Shelf. *Deep-Sea Research Part II*, *147*, 58–68. https://doi.org/10.1016/j.dsr2.2017.04.023

Blood, D. M., Matarese, A. C., & Yoklavich, M. M. (1994). Embryonic development of walleye pollock, *Theragra chalcogramma*, from Shelikof Strait, Gulf of Alaska. *Fishery Bulletin US*, *92*, 207–222.

Bond, N. A., Cronin, M. R., Freeland, H., & Mantua, N. (2015). Causes and impacts of the 2014 warm anomaly in the NE Pacific. *Geophysical Research Letters*, *42*, 3414–3420. https://doi.org/10.1002/2015GL063306

Brodeur, R. D., & Wilson, M. T. (1996). A review of the distribution, ecology and population dynamics of age- 0 walleye pollock in the Gulf of Alaska. *Fisheries Oceanography*, *5*(Suppl. 1), 148–166. https://doi.org/10.1111/j.1365-2419.1996.tb00089.x

Brown, A. L., Mier, K. L., & Busby, M. S. (2001). Walleye pollock *Theragra chalcogramma* during transformation from the larval to juvenile stage: Otolith and osteological development. *Marine Biology*, *139*, 845–851. https://doi.org/10.1007/s002270100641

Buchheister, A., Wilson, M. T., Foy, R. J., & Beauchamp, D. A. (2006). Seasonal and geographic variation in condition of juvenile walleye pollock in the western Gulf of Alaska. *Transactions of the American Fisheries Society*, *135*, 897–907. https://doi.org/10.1577/T05-105.1

Chan, K.-S., Zhang, T., & Bailey, K. M. (2010). Otolith biochronology reveals factors underlying dynamics in marine fish larvae. *Marine Ecology Progress Series*, *412*, 1–10. https://doi.org/10.3354/meps08698

Ciannelli, L., Bailey, K. M., Chan, K.-S., Belgrano, A., & Stenseth, N. C. (2005). Climate change causing phase transitions of walleye pollock (*Theragra chalcogramma*) recruitment dynamics. *Proceedings of the Royal Society B*, *272*, 1735–1743.

Ciannelli, L., Chan, K.-S., Bailey, K. M., & Stenseth, N. C. (2004). Nonadditive effects of the environment on the survival of a large marine fish population. *Ecology*, *85*, 3418–3427. https://doi.org/10.1890/03-0755

Cowen, R. K., Gawarkiewicz, G., Pineda, J., Thorrold, S. R., & Werner, F. E. (2007). Population connectivity in marine systems an overview. *Oceanography*, *20*, 14–21. https://doi.org/10.5670/oceanog.2007.26

Davis, M. (2001). Behavioral responses of walleye pollock, *Theragra Chalcogramma*, larvae to experimental gradients of sea water flow: Implications for vertical distribution. *Environmental Biology of Fishes*, *61*, 253–260. https://doi.org/10.1023/A:1010947621672

Dorn, M., Aydin, K., Fissel, B., Palsson, W., Spalinger, K., Stienessen, S., … Zador, S. (2018). Assessment of the walleye pollock stock in the Gulf of Alaska. In *Stock assessment fishery evaluation report for the groundfish resources of the Gulf of Alaska* (pp. 1–130). Anchorage, AK: North Pacific Fishery Management Council.

Dougherty, A. B., Bailey, K. M., & Mier, K. L. (2007). Interannual differences in growth and hatch date distribution of age-0 year walleye pollock *Theragra chalcogramma* (Pallas) sampled from the Shumagin Islands region of the Gulf of Alaska, 1985–2001. *Journal of Fish Biology*, *71*, 763–780.

Dougherty, A., Bailey, K., Vance, T., & Cheng, W. (2012). Underlying causes of habitat-associated differences in size of age-0 walleye pollock (*Theragra chalcogramma*) in the Gulf of Alaska. *Marine Biology*, *159*, 733–1744. https://doi.org/10.1007/s00227-012-1961-2

Dougherty, A., Deary, A., & Rogers, L. (2019). Rapid larval assessment in the Gulf of Alaska. In S. Zador, E. Yasumiishi, & G. A. Whitehouse (Eds.), *Ecosystem Status Report 2019: Gulf of Alaska*, *Stock Assessment and Fishery Evaluation Report* (pp. 94–97). Anchorage, AK: North Pacific Fishery Management Council.

Doyle, M. J., & Mier, K. M. (2016). Early life history pelagic exposure profiles of selected commercially important fish species in the Gulf of Alaska. *Deep-Sea Research Part II*, *132*, 162–193. https://doi.org/10.1016/j.dsr2.2015.06.019

Doyle, M. J., Strom, S. L., Coyle, K. O., Hermann, A. J., Ladd, C., Matarese, A. C., … Hopcroft, R. R. (2019). Early life history phenology among Gulf of Alaska fish species: Strategies, synchronies, and sensitivities. *Deep-Sea Research Part II*, *165*, 41–73. https://doi.org/10.1016/j.dsr2.2019.06.005

Duffy-Anderson, J. T., Bailey, K. M., & Ciannelli, L. (2002). Consequences of a superabundance of larval walleye pollock *Theragra chalcogramma* in the Gulf of Alaska in 1981. *Marine Ecology Progress Series*, *243*, 179–190. https://doi.org/10.3354/meps243179

Endo, C. A. K., Vikebø, F. B., Yaragina, N. A., Hjøllo, S. S., & Stige, L. C. (2020). Effects of climate and spawning stock structure on the spatial distribution of Northeast Arctic cod larvae. *ICES Journal of Marine Science*. https://doi.org/10.1093/icesjms/fsaa057

Fox, J., & Weisberg, S. (2019). *An R companion to applied regression* (3rd ed.). Thousand Oaks, CA: Sage.

Hare, J. A. (2014). The future of fisheries oceanography lies in the pursuit of multiple hypotheses. *ICES Journal of Marine Science*, *71*, 2343–2356. https://doi.org/10.1093/icesjms/fsu018

Hermann, A. J., Hinckley, S., Megrey, B. A., & Stabeno, P. J. (1996). Interannual variability of the early life history of walleye pollock near Shelikof Strait as inferred from a spatially explicit, individual-based model. *Fisheries Oceanography*, *5*(Suppl. 1), 39–57. https://doi.org/10.1111/j.1365-2419.1996.tb00081.x

Hinckley, S., Bailey, K. M., Picquelle, S. J., Schumacher, J. D., & Stabeno, P. J. (1991). Transport, distribution, and abundance of larval and juvenile walleye pollock (*Theragra chalcogramma*) in the western Gulf of Alaska. *Canadian Journal of Fisheries and Aquatic Sciences*, *48*, 91–98.

Hinckley, S., Bailey, K., Picquelle, S., Yoklavich, M., & Stabeno, P. (1993). Age-specific mortality and transport of larval walleye pollock *Theragra chalcogramma* in the western Gulf of Alaska. *Marine Ecology Progress Series*, *98*, 17–29. https://doi.org/10.3354/meps098017

Hinckley, S., Hermann, A. J., Mier, K. L., & Megrey, B. A. (2001). Importance of spawning location and timing to successful transport to nursery areas: A simulation study of Gulf of Alaska walleye pollock. *ICES Journal of Marine Science*, *58*, 1042–1052. https://doi.org/10.1006/jmsc.2001.1096

Houde, E. D. (2008). Emerging from Hjort's Shadow. *Journal of Northwest Atlantic Fishery Science*, *41*, 53–70. https://doi.org/10.2960/J.v41.m634

Huse, G. (2016). A spatial approach to understanding herring population dynamics. *Canadian Fisheries and Aquatic Sciences*, *73*, 177–188. https://doi.org/10.1139/cjfas-2015-0095

Incze, L. S., Kendall, A. W. Jr, Schumacher, J. D., & Reed, R. K. (1989). Interactions of a mesoscale patch of larval fish (*Theragra chalcogramma*) with the Alaska Coastal Current. *Continental Shelf Research*, *9*, 269–284. https://doi.org/10.1016/0278-4343(89)90028-9

Kendall, A. W., Jr., Incze, L. S., Ortner, P. B., Cummings, S. R., & Brown, P. K. (1994). The vertical distribution of eggs and larvae of walleye pollock, *Theragra chalcogramma*, in Shelikof Strait, Gulf of Alaska. *Fishery Bulletin US*, *92*, 540–554.

Knickle, D. C., & Rose, G. A. (2010). Seasonal spawning and wind-regulated retention-dispersal of early life stage Atlantic cod (*Gadus morhua*) in a Newfoundland fjord. *Fisheries Oceanography*, *19*, 397–411. https://doi.org/10.1111/j.1365-2419.2010.00553.x

Ladd, C., & Bond, N. A. (2002). Evaluation of the NCEP-NCAR Reanalysis in the Northeast Pacific and the Bering Sea. *Journal of Geophysical Research*, *107*(C10), 3158. https://doi.org/10.1029/2001JC001157

Ladd, C., Cheng, W., & Salo, S. (2016). Gap Winds near Kodiak Island, Alaska and effects on regional oceanography. *Deep-Sea Research II*, *132*, 54–67. https://doi.org/10.1016/j.dsr2.2015.08.005

Ladd, C., Stabeno, P., & Cokelet, E. D. (2005). A note on cross-shelf exchange in the northern Gulf of Alaska. *Deep-Sea Research II*, *52*, 667–679. https://doi.org/10.1016/j.dsr2.2004.12.022

Lee, Y.-W., Megrey, B. A., & Macklin, S. A. (2009). Evaluating the performance of Gulf of Alaska walleye pollock (*Theragra chalcogramma*) recruitment forecasting models using a Monte Carlo resampling strategy. *Canadian Journal of Fishery and Aquatic Science*, *66*, 367–381. https://doi.org/10.1139/F08-203

Litzow, M. A., Ciannelli, L., Puerta, P., Wettstein, J. J., Rykaczewski, R. R., & Opiekun, M. (2019). Nonstationary environmental and community relationships in the North Pacific Ocean. *Ecology*, *100*, e02760. https://doi.org/10.1002/ecy.2760

Matta, M. E., & Kimura, D. K. (Eds.) (2012). *Age determination manual of the Alaska Fisheries Science Center Age and Growth Program* (p. 13). NOAA Professional Paper, NMFS 13.

Mazur, M. M., Wilson, M. T., Dougherty, A. B., Buchheister, A., & Beauchamp, D. A. (2007). Temperature and prey quality effects on growth of juvenile walleye pollock *Theragra chalcogramma* (Pallas): A spatially explicit bioenergetics approach. *Journal of Fish Biology*, *70*, 816–836. https://doi.org/10.1111/j.1095-8649.2007.01344.x

Megrey, B. A., Hollowed, A. B., Hare, S. R., Macklin, S. A., & Stabeno, P. J. (1996). Contributions of FOCI research to forecasts of year-class strength of walleye pollock in Shelikof Strait. *Alaska. Fisheries Oceanography*, *5*(Suppl. 1), 189–203. https://doi.org/10.1111/j.1365-2419.1996.tb00092.x

Meuter, F. J., & Norcross, B. L. (2002). Spatial and temporal patterns in the demersal fish community on the shelf and upper slope regions of the Gulf of Alaska. *Fishery Bulletin*, *100*, 559–581.

Mordy, C. W., Stabeno, P. J., Kachel, N. B., Kachel, D., Ladd, C., Zimmermann, M., … Doyle, M. J. (2019). Patterns of flow in the canyons of the northern Gulf of Alaska. *Deep-Sea Research II*, *165*, 203–220. https://doi.org/10.1016/j.dsr2.2019.03.009

Parada, C., Hinckley, S., Horne, J., Mazur, M., Hermann, A., & Curchister, E. (2016). Modeling connectivity of walleye pollock in the Gulf of Alaska: Are there any linkages to the Bering Sea and Aleutian Islands? *Deep-Sea Research II*, *132*, 227–239. https://doi.org/10.1016/j.dsr2.2015.12.010

Porter, S. M., Ciannelli, L., Hillgruber, N., Bailey, K. M., Chan, K.-S., Canino, M. F., & Haldorson, L. J. (2005). Environmental factors influencing larval walleye pollock *Theragra chalcogramma* feeding in Alaskan waters. *Marine Ecology Progress Series*, *302*, 207–217. https://doi.org/10.3354/meps302207

R Core Team (2019). *R: A language and environment for statistical computing*. Vienna, Austria: R Foundation for Statistical Computing.

Reed, R. K., & Schumacher, J. D. (1986). Physical oceanography. In D. W. Hood, & S. T. Zimmerman (Eds.), *The Gulf of Alaska: Physical environment and biological resources* (pp. 57–75). Washington, DC: Ocean Assessment Division, NOAA.

Reed, R. K., Schumacher, J. D., & Incze, L. S. (1987). Circulation in Shelikof Strait, Alaska. *Journal of Physical Oceanography*, *17*, 1546–1554. https://doi.org/10.1175/1520-0485(1987)017<1546:CISSA>2.0.CO;2

Rogers, L. A., & Dougherty, A. B. (2019). Effects of climate and demography on reproductive phenology of a harvested marine fish population. *Global Change Biology*, *25*, 708–720. https://doi.org/10.1111/gcb.14483

Rogers, L. A., Wilson, M. T., Duffy-Anderson, J. T., Kimmel, D. G., & Lamb, J. (2020). Pollock and 'the Blob': Impacts of a marine heatwave on walleye pollock early life stages. *Fisheries Oceanography*, https://doi.org/10.1111/fog.12508

Rogers, L., Wilson, M., & Porter, S. (2019). Abundance of YOY pollock and capelin in western Gulf of Alaska. In S. Zador, E. Yasumiishi, & G. A. Whitehouse (Eds.), *Ecosystem Status Report 2019: Gulf of Alaska*, *Stock Assessment and Fishery Evaluation Report* (pp. 102–105). Anchorage, AK: North Pacific Fishery Management Council.

Rogers-Cotrone, J., Yankovsky, A. E., & Weingartner, T. J. (2008). The impact of spatial wind variations on freshwater transport by the Alaska Coastal Current. *Journal of Marine Research*, *66*, 899–925. https://doi.org/10.1357/002224008788064603

Romagnoni, G., Kvile, K. Ø., Dagestad, K.-F., Eikeset, A. M., Kristiansen, T., Stenseth, N. C., & Langangen, Ø. (2020). Influence of larval transport and temperature on recruitment dynamics of North Sea cod (*Gadus morhua*) across spatial scales of observation. *Fisheries Oceanography*, *29*, 324–339. https://doi.org/10.1111/fog.12474

Schlaefer, J. A., Wolanksi, E., Lambrechts, J., & Kingsford, M. J. (2018). Wind conditions on the Great Barrier Reef influenced the recruitment of snapper (*Lutjanus carponotatus*). *Frontiers in Marine*, *5*, 1–20. https://doi.org/10.3389/fmars.2018.00193

Schumacher, J. D., & Reed, R. K. (1980). Coastal flow in the northwest Gulf of Alaska: The Kenai Current. *Journal of Geophysical Research*, *85*, 6680–6688. https://doi.org/10.1029/JC085iC11p06680

Schumacher, J. D., & Reed, R. K. (1986). On the Alaska Coastal Current in the western Gulf of Alaska. *Journal of Geophysical Research*, *91*, 9655–9661. https://doi.org/10.1029/JC091iC08p09655

Shanks, A. L., & Eckert, G. L. (2005). Population persistence of California Current fishes and benthic crustaceans: A marine drift paradox. *Ecological Monographs*, *75*, 505–524. https://doi.org/10.1890/05-0309

Shieh, G. (2019). Effect size, statistical power, and sample size for assessing interactions between categorical and continuous variables. *British Journal of Mathematical and Statistical Psychology*, *72*, 136–154. https://doi.org/10.1111/bmsp.12147

Shima, M., Hollowed, A. B., & VanBlaricom, G. R. (2002). Changes over time in the spatial distribution of walleye pollock (*Theragra chalcogramma*) in the Gulf of Alaska, 1984–1996. *Fishery Bulletin US*, *100*, 307–323.

Sorte, C. J. B. (2013). Predicting persistence in a changing climate: Flow direction and limitations to redistribution. *Oikos*, *122*, 161–170. https://doi.org/10.1111/j.1600-0706.2012.00066.x

Stabeno, P. J., Bell, S., Cheng, W., Danielson, S., Kachel, N. B., & Mordy, C. W. (2016). Long-term observations of Alaska Coastal Current in the northern Gulf of Alaska. *Deep-Sea Research II*, *132*, 24–40. https://doi.org/10.1016/j.dsr2.2015.12.016

Stabeno, P. J., Bond, N. A., Hermann, A. J., Kachel, N. B., Mordy, C. W., & Overland, J. E. (2004). Meteorology and oceanography of the northern Gulf of Alaska. *Continental Shelf Research*, *24*, 859–897. https://doi.org/10.1016/j.csr.2004.02.007

Stabeno, P. J., Schumacher, J. D., Bailey, K. M., Brodeur, R. D., & Cokelet, E. D. (1996). Observed patches of walleye pollock eggs and larvae in Shelikof Strait, Alaska: Their characteristics, formation and persistence. *Fisheries Oceanography*, *5*(Suppl. 1), 81–91. https://doi.org/10.1111/j.1365-2419.1996.tb00084.x

von Szalay, P. G., & Raring, N. W. (2018). *Data Report: 2017 Gulf of Alaska bottom trawl survey*. U.S. Department of Commerce, NOAA Technical Memorandum, NMFS-AFSC-374.

Wespestad, V. G., Fritz, L. W., Ingraham, W. J., & Megrey, B. A. (2000). On relationships between cannibalism, climate variability, physical transport, and recruitment success of Bering Sea walleye pollock (Theragra chalcogramma). *ICES Journal of Marine Science*, *57*, 268–274. https://doi.org/10.1006/jmsc.2000.0640

Wilson, M. T. (2000). Effects of year and region on the abundance and size of age-0 walleye pollock, *Theragra chalcogramma*, in the western Gulf of Alaska, 1985–1988. *Fishery Bulletin US*, *98*, 823–834.

Wilson, M. T. (2009). Ecology of small neritic fishes in the western Gulf of Alaska. I. Geographic distribution in relation to prey density and the physical environment. *Marine Ecology Progress Series*, *392*, 223–237.

Wilson, M. T., Brodeur, R. D., & Hinckley, S. (1996). Distribution and abundance of age-0 walleye pollock, Theragra chalcogramma, in the western Gulf of Alaska during September 1990. In R. D. Brodeur, P. A. Livingston, T. R. Loughlin, & A. B. Hollowed (Eds.), *Ecology of juvenile walleye pollock*, Theragra chalcogramma (pp. 11–24). U.S. Department of Commerce, NOAA Technical Report, NMFS 126.

Wilson, M. T., Buchheister, A., & Jump, C. (2011). Regional variation in the annual feeding cycle of juvenile walleye pollock (*Theragra chalcogramma*) in the western Gulf of Alaska. *Fishery Bulletin US*, *109*, 316–326.

Wilson, M. T., Dougherty, A., Matta, M. E., Mier, K. L., & Miller, J. A. (2018). Otolith chemistry of juvenile walleye pollock *Gadus chalcogrammus* in relation to regional hydrography: Evidence of spatially split cohorts. *Marine Ecology Progress Series*, *588*, 163–178. https://doi.org/10.3354/meps12425

Wilson, M. T., Mier, K. L., & Jump, C. M. (2013). Effect of region on the food-related benefits to age-0 walleye pollock (*Theragra chalcogramma*) in association with midwater habitat characteristics in the Gulf of Alaska. *ICES Journal of Marine Science*, *70*, 1396–1407. https://doi.org/10.1093/icesjms/fst138

Yankovsky, A. E., Maze, G. M., & Weingartner, T. J. (2010). Offshore transport of the Alaska Coastal Current water induced by a cyclonic wind field. *Geophysical Research Letters*, *37*, 1–5. https://doi.org/10.1029/2009GL041939

Zhang, T., Bailey, K. M., & Chan, K.-S. (2010). Recruitment forecast models for walleye pollock *Theragra chalcogramma* fin-tuned from juvenile survey data, predator abundance and environmental phase shifts. *Marine Ecology Progress Series*, *417*, 237–248.

SUPPORTING INFORMATION

Additional supporting information may be found online in the Supporting Information section.

How to cite this article: Wilson MT, Laman N. Interannual variation in the coastal distribution of a juvenile gadid in the northeast Pacific Ocean: The relevance of wind and effect on recruitment. *Fish Oceanogr.* 2021;30:3–22. https://doi.org/10.1111/fog.12499